Weierstraß-Institut

für Angewandte Analysis und Stochastik

Leibniz-Institut im Forschungsverbund Berlin e. V.

Preprint ISSN 0946 – 8633

Modulation instability in filamentary self-compression

Carsten Brée[1,2] Ayhan Demircan[1], Günter Steinmeyer[2,3]

submitted: December 21, 2010

[1] Weierstrass Institute for Applied Analysis and Stochastics, Mohrenstraße 39, 10117 Berlin, Germany

[2] Max Born Institute for Nonlinear Optics and Short Pulse Spectroscopy, Max-Born-Straße 2A, 12489 Berlin, Germany

[3] Optoelectronics Research Centre, Tampere University of Technology, 33101 Tampere, Finland

No. 1570

Berlin 2010

2010 *Mathematics Subject Classification.* Primary 78A60.

2010 *Physics and Astronomy Classification Scheme.* 42.65.-k,42.65.Jx,42.65.Re, 42.65.Sf.

Key words and phrases. Nonlinear Optics, Modulation instability, Femtosecond Filamentation, Pulse compression.

Financial support by the Deutsche Forschungsgemeinschaft, grants DE 1209/1-2 and STE 762/7-2, is gratefully acknowledged. GS gratefully acknowledges support by the Academy of Finland (project grant 128844).

Edited by
Weierstraß-Institut für Angewandte Analysis und Stochastik (WIAS)
Leibniz-Institut im Forschungsverbund Berlin e. V.
Mohrenstraße 39
10117 Berlin
Germany

Fax: +49 30 2044975
E-Mail: preprint@wias-berlin.de
World Wide Web: http://www.wias-berlin.de/

Abstract

We numerically analyze filamentary propagation for various medium- and input pulse parameters and show that temporal self-compression can greatly benefit from refocusing events. Analyzing the dynamical behavior in the second focal spot, it turns out that a dispersive temporal break-up may appear due to the emission of a hyperbolic shock-wave from the self-steepened trailing edge of the pulse. This break-up event enhances the self-compression capabilities of laser filaments, enabling up to 12-fold temporal compression. Only slightly perturbing the input pulse parameters, we further identify a regime in which refocusing events give rise to extended subdiffractive propagation in a weakly ionized channel.

1 Introduction

Filamentary pulse compression [1] has emerged as an alternative to hollow-fiber compression [2] of laser pulses. Not being limited by potential damage of the guiding structure, propagation of multi-mJ pulses in self-guided filaments provides sufficient spectral broadening to generate 5 fs pulses with subsequent chirped mirror dispersion compression [3]. Removing the need for a well-balanced dispersion compensation step, filaments have also been demonstrated to provide pure self-compression of 45 fs pulses well into the sub-10 fs range [4]. This remarkably simple process has subsequently been analyzed to occur in three steps [5, 6, 7], involving an initial plasma-induced pulse break-up, isolation of one of the fragments and subsequent compression of the latter upon further propagation. This scheme was later generalized [8] by noting that a refocusing event in the postionization regime of the filament can yield an additional temporal break-up event, enabling more than tenfold compression. However, considering experimental applications of filamentary self-compression, it is known that filamentation suffers from several instabilities. In fact, the Benjamin-Feir instability [9] of deep-water waves may be regarded as a prototypical example of a variety of instabilities arising in nonlinear optical systems, especially in femtosecond filaments. In the spatial domain, it is known that an initially radially symmetric beam is subject to an azimuthal modulation instability (MI) [10] and breaks up into multiple filaments. This instability can rather easily be avoided by choosing input powers not exceeding $\approx 5P_{\mathrm{cr}}$ [4], where $P_{\mathrm{cr}} = \lambda^2/2\pi n_0 n_2$ is the critical power for Kerr self-focusing. The latter effect is a major ingredient to the theory of filamentation. It is known to provide an additional source of instability, as the evolution equations used for modeling self-focusing admit solutions that blow-up at finite propagation distances [11]. However, plasma defocusing is able to counteract the Kerr induced collapse, giving rise to the phenomenon of intensity clamping [12]. In fact, it has recently been demonstrated that the clamped intensity is remarkably stable against variations of the input peak

power of the pulse laser beam [13]. Considering the interplay of group-velocity dispersion (GVD) and self-focusing, a spatiotemporal modulation instability can be observed, leading to both, the prediction of temporal pulse splitting [14] and that of spatiotemporally coupled structures such as hyperbolic shock waves, X-waves and conical emission (CE) [15, 16]. We analyze the impact of the self-focusing instability and X-wave related MI on filamentary self-compression in various self-compression regimes discussed in [7, 6, 8] and show that filamentation regimes exist which are strongly sensitive to input noise.

2 Modeling

For the investigation of self-compression induced by multiple pulse breaking, we perform numerical simulations of the generalized Nonlinear Schrödinger equation, which couples the envelope $\mathcal{E}$ of the electric field to the plasma density ρ of the medium [5] according to

$$\begin{aligned} \partial_z \mathcal{E} &= \frac{i}{2k_0} T^{-1} \Delta_\perp \mathcal{E} + i\mathcal{D}\mathcal{E} + i\frac{\omega_0}{c} n_2 T |\mathcal{E}|^2 \mathcal{E} \qquad (1) \\ &- i\frac{k_0}{2\rho_c} T^{-1} \rho \mathcal{E} - \frac{\sigma}{2}\rho\mathcal{E} - \frac{U_i W(I)(\rho_{nt}-\rho)}{2I}\mathcal{E}, \\ \partial_t \rho &= W(I)(\rho_{nt}-\rho) + \frac{\sigma}{U_i}\rho I\,, \qquad (2) \end{aligned}$$

where $I = |\mathcal{E}|^2$ is the cycle-averaged field intensity. Assuming cylindrical symmetry, the transverse Laplacian reduces to $\Delta_\perp = (1/r)\partial_r r \partial_r$, with $r = (x^2+y^2)^{1/2}$ in cylindrical coordinates. Space-time focusing and self-steepening are introduced by the operator $T = 1 + \frac{i}{\omega_0}\partial_t$, the operator T^{-1} being evaluated in the Fourier domain. Correspondingly, the operator $\mathcal{D}$ modeling dispersion in argon is treated in the Fourier domain according to

$$\tilde{\mathcal{D}}(\omega) = k(\omega) - k_0 - (\omega-\omega_0)\frac{\partial_k}{\partial_\omega}|_{\omega=\omega_0} \qquad (3)$$

where $k(\omega) = n(\omega)\omega/c$ is the wavenumber at the angular frequency ω, and $n(\omega)$ is the frequency dependent refractive index in argon according to Ref. [17]. The carrier frequency of the laser field and corresponding wavenumber are denoted by ω_0 and k_0, respectively, with a carrier wavelength $\lambda = 800$ nm. n_2 is the nonlinear refractive index [18] and U_i corresponds to the ionization potential of the medium. Moreover, $\rho_c = 1.73 \times 10^{21}$ cm^{-3} is the critical plasma density at ω_0, and ρ_{nt} denotes the neutral density of the medium. σ is the cross section for collisional ionization. The ionization rate $W(I)$ is modeled according to Perelomov-Popov-Terent'ev (PPT) [19] and adequately describes both multi-photon and tunneling ionization processes.

Equations (1) and (2) are numerically integrated by means of a parallel split-step radial code for pulses propagation in combination with a Runge-Kutta scheme for the nonlinear part and a Crank-Nicholson scheme for the radial part [20].

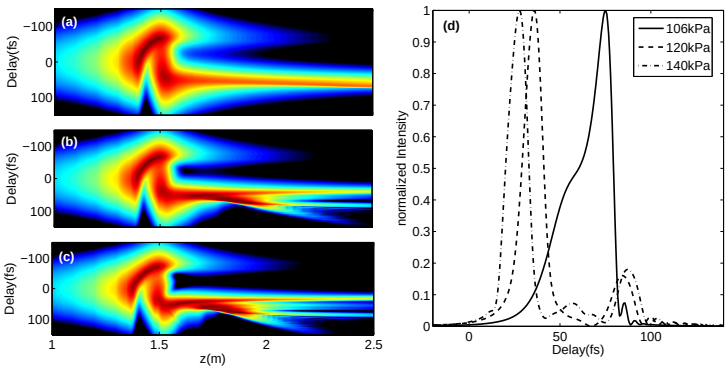

Figure 1: Evolution of the on-axis intensity profile along z for (a) $p = 106, (b)120$ and (c) 140 kPa, covering single- and double self-compression regimes of filamentation. (d) Corresponding evolution of the temporal pulse width for the various pressures.

3 Double self-compression in argon

Assuming an $f = 1.5$ m lens, we simulate focusing of 2.5 mJ input pulses at 800 nm with a beam waist $w_0 = 3.5$ mm and pulse duration $t_{\mathrm{FWHM}} = 120$ fs into the medium at gas pressures of $p = 106$, 120 and 140 kPa for fixed input pulse parameters. The self-compressed pulses emerging from these different scenarios are referred to as pulse I, II and III, respectively. Figure 1(a) shows the self-compression dynamics described in [7] for the generation of one well isolated few-cycle pulse. For an efficient exploitation of this scheme, a cascaded version of this dynamics can be obtained by slightly increasing the pressure to $p = 120$ kPa [see Fig. 1(b)], as it has already been show in [8]. However, a delicate balance between the different parameters is necessary to benefit from cascaded self-compression. As can be seen in Fig. 1(c), a slight change of only one parameter completely changes the dynamics so that it is difficult to achieve one isolated pulse. In Fig. 1(d), the on-axis temporal profiles for the different scenarios are depicted. Clearly, the pulses emerging from the two-foci scenario are considerably shorter than the self-compressed pulse in the single-focus regime (15 fs vs. 25 fs). However, as is evident both from Fig. 1(c) and (d), increasing the pressure is accompanied by a growing tendency of multiple pulse splitting. Indeed, pulses II and III show a pronounced trailing sub-pulse, which is often undesirable in applications. So far, we have restricted our discussion to the temporal domain, in which both focusing events appear to have a similar compressing effect on the pulse duration. Comparing spectra obtained in both regimes [Fig. 2(a)], however, it becomes noticeable that the pronounced blue wing of the spectrum is strongly suppressed when the pressure is increased from 106 to 120 kPa. Instead, new spectral components appear on the long-wavelength side of the spectrum. In consequence, the spectra emerging from the double self-compression regime exhibit an overall red-shift. Figure 2(b) shows spatially resolved XFROG traces for pulse I, indicating the spectro-temporal energy distribution inside the pulse. On-axis, a characteristic mirrored Γ-shape is observed, which is a consequence of self-steepening and leads to a pronounced spectral blue-shift in the trailing edge of the pulse. It is also evident that in this scheme, self-compression and spectral broadening towards blue frequencies is only efficient on-axis,

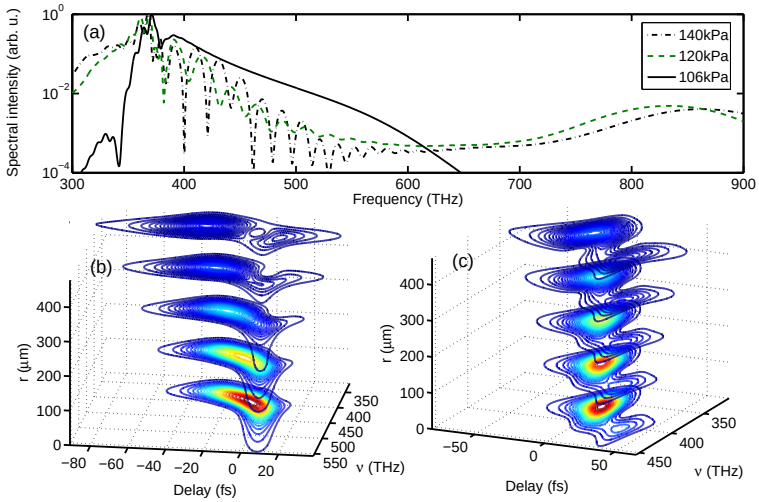

Figure 2: (a) Spectra of filamentary self-compressed pulses, $p = 106$ (solid line) 120 (dashed line) and 140 kPa (dashed-dotted line). (b) spatially resolved XFROG trace of the filament pulse capture at $z = 2.5$ m in the single self-compression regime, $p = 106$ kPa. (c) (b) spatially resolved XFROG trace of the filament pulse capture at $z = 2.5$ m in the double self-compression regime, $p = 120$ kPa.

giving rise to a spatially inhomogeneous structure of the pulse. The corresponding spatially resolved XFROG trace for pulse II is shown in Fig. 2(c). From this trace it is evident that the trailing sub-pulse is red-shifted with respect to the main pulse. This behavior is contrasted by the small red leading sub-pulse mainly observed in filament self-compression experiments. However, the emergence of the red trailing sub-pulse in the two-foci scenario was experimentally confirmed in [8]. Considering the spatial structure of pulse II and comparing it to that of pulse I, a more homogeneous structure is found, as is obvious from Fig. 2(d). As discussed in Ref. [8], this shows that the self-compression scheme in which pulse II is generated is in favor of more energetic pulses.

4 Impact of the modulation instability

Due to the fact that our compression scheme relies on cascading break-up events and the rapid diffraction of undesired sub-pulses, the usefulness of this scheme strongly depends on the fine-tuning of the initial and medium parameters. In particular, the process is strongly sensitive to input noise. To demonstrate this, we we add 0.5% amplitude noise to pulse I ($p = 106$ kPa) and simulate several shots with identical initial conditions except for the noise added. The results of these simulations are summarized in Figs. 3(a) and (b) for five arbitrarily selected simulation results. Figure 3(a) shows the evolution of the peak intensity of the pulse along z. Both the peak intensity in the second focus and its z-position are subject to strong variations. Consequently, the output pulse profiles at $z = 2.5$ m shown in Fig. 3(b) exhibit large shot-to-shot fluctuations induced by the input noise. The observed pulse durations vary between 25 and 40 femtosec-

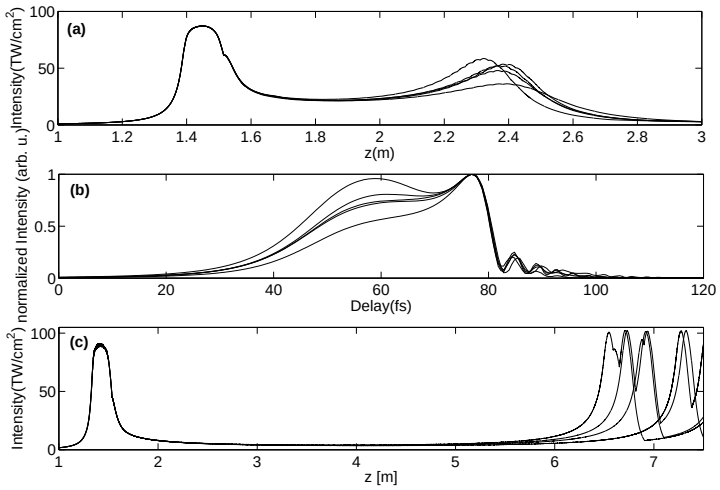

Figure 3: (a) Evolution of peak intensity, five shots with identical initial conditions (except noise), $p = 106\,\mathrm{kPa}$. (b) Corresponding pulse shapes at $z = 2.5\,\mathrm{m}$. (c) Same as (a), but GVD and T eliminated from the evolution Eq. (1).

onds, an amount that cannot be neglected experimentally and is expected to strongly affect possible applications of filamentary self-compressed few-cycle pulses.

Note that in the corresponding simulations where pulse I was propagated without added noise, a second focus was completely absent. Thus, the presence of an inherent instability which amplifies initial noise appears plausible. A possible origin of this instability has been discussed in Ref. [8], namely the modulation instability arising from the interplay of normal group velocity dispersion (GVD) and Kerr self-focusing. This instability is known to give rise to X-wave formation and conical emission (CE) [16, 21], where the latter effect can alternatively be described in terms of a simple interference model [22]. According to theoretical results of [14, 15], the instability arising from the interplay of self-focusing and normal GVD has been discussed as being responsible for the pulse break-up occurring in the second focus [8]. Indeed, it was found that angle-resolved far-field spectra of the pulses after the second focus show a characteristic signature of this spatio-temporal modulation instability. Here, Fig. 4 shows corresponding color-coded information in the (t, θ)-plane, where t is the time-delay of the laser pulse and $\theta \approx k_\perp/|\vec{k}|$, with $k = (k_x, k_y, k_z)$ being the wave-vector and $k_\perp = \sqrt{k_x^2 + k_y^2}$. Again, the hyperbola appearing at positive delay is a clear indication of the X-wave related spatio-temporal modulation instability. Figure 4(b) shows an angle spectrum at $t = 250\,\mathrm{fs}$ in the trailing part of the pulse, with characteristic, MI-induced side lobes in the spectrum.

The major ingredient to any theory on filamentation, Kerr self-focusing, serves as a further source of instability. In the theory of self-focusing, it is known that any solution ψ of the Nonlinear Schrödinger equation in $2 + 1$ dimensions either decays or blows-up at finite propagation distances, depending whether or not the L_2-norm of the solution exceeds a certain critical value. Indeed, in the theory of self-focusing of laser beams, this value corresponds to the critical power $P_{\mathrm{cr}} = \lambda^2/(2\pi n_0 n_2)$. A stationary solution to the problem of optical self-focusing described by the Nonlinear Schrödinger equation has been derived in Ref. [23]. However, this so-called

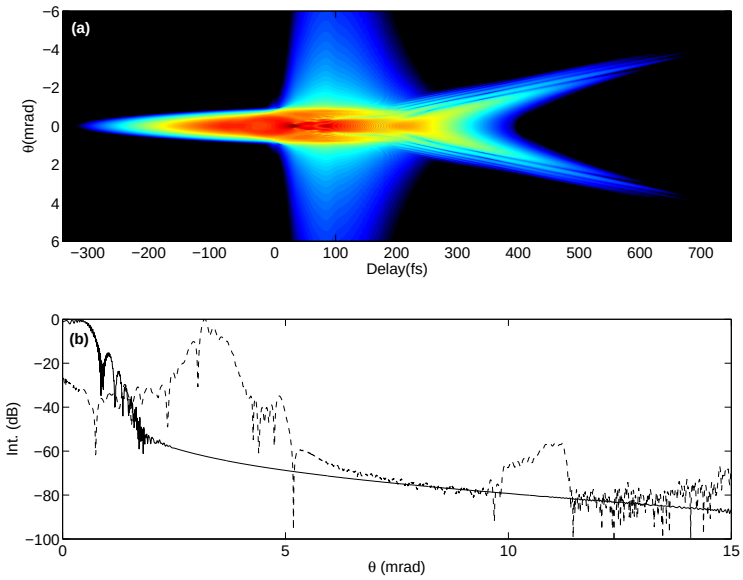

Figure 4: (a) Intensity distribution of a self-compressed pulse at $z = 2.5$ m, $p = 120$ kPa in the (t, θ)-plane. (b) Two slices of the angle-spectrum, normalized to unity, at $t = 250$ fs (solid line) and $t = 400$ fs (dashed line), with characteristic side lobes induced by MI.

Townes-soliton is not a stable one, as any small perturbation of the stationary shape leads to decay or blow-up. Eliminating dispersion by setting $\mathcal{D} = 0$ and any other temporal coupling effects by setting $T = 1$ in Eq. (1), a second set of simulations is performed in order to analyze the noise-dependence of self-focusing. Again, 2.5 mJ pulses at $p = 106$ kPa are used as initial condition. However, with unchanged initial beam waist, the pulses only form a small-scale filament in the immediate vicinity of the nonlinear focus and rapidly diffract afterwards. Thus, in order to observe a high-intensity post-ionization regime and refocusing events, the initial beam waist is changed to $w_0 = 2.7$ mm. With this modification of initial conditions, it is again possible to observe the desired post-ionization dynamics and a refocusing stage as shown in Fig. 4(c). Note that for these parameters, the distance between the foci is strongly enlarged, with a 5 m long, plasma-less filament channel with nearly constant intensity in between. Again, 0.5% of input noise lead to even stronger fluctuations of the refocusing stage after the first nonlinear focus. We therefore conclude that the spatio-temporal coupling induced by GVD, leading to the phenomenon of X-waves and CE, is not relevant for the observed fluctuations of the second focus. Rather, the well-known self-focusing instability suffices to explain the observed fluctuations. We wish to emphasize that we performed additional simulations (not shown) that revealed that the sensitivity to noise is particularly pronounced in the transition regime between scenarios I and II, i.e., for pressures equal to or slightly higher than 1.06 kPa.

5 Conclusion

In conclusion, we have shown that the cascaded self-compression scheme of [8] is affected by modulation instabilities in a two-fold way: first, as already shown in the latter work, the temporal break-up emerging in the second focus can be traced back to the spatiotemporal MI due to the interplay of GVD and self-focusing. This is also known to be responsible for the spontaneous formation of X-waves and conical emission. Second, in the current article we observed that the refocusing dynamics is strongly affected by input noise, giving rise to fluctuations of the output pulse temporal profiles. This noise sensitivity is especially strong in the transitory regime between the single- and the double self-compression scenarios, where our simulations revealed that variations of more than 50% are to be expected. Concerning experimental applications of self-compression, it therefore seems to be indicated to avoid this transitory regime, operating rather in scenario II discussed here, splitting. In addition, by fine-tuning of the initial laser pulse parameters, our simulations indicate the possiblity of a refocusing event with significant plasma generation in the second focus, comparable to that obtained in the first focus. From this , applications like high-order harmonics generation induced by filamentary pulses [24] and THz generation [25, 26] may possibly benefit. Nevertheless, care must be taken to avoid unwanted multiple temporal splittings which tend to occur in this cascaded scheme.

References

[1] C. P. Hauri, W. Kornelis, F. W. Helbing, A. Heinrich, A. Couairon, A. Mysyrowicz, J. Biegert, U. Keller, Appl. Phys. B **79**, 673 (2004).

[2] M. Nisoli, S. De Silvestri, O. Svelto, R. Szipőcs, K. Ferencz, C. Spielmann, S. Sartania, and F. Krausz, Opt. Lett. **22**, 522 (1997).

[3] A. Couairon, M. Franco, A. Mysyrowicz, J. Biegert, and U. Keller, Opt. Lett. **30**, 2657–2659 (2005).

[4] G. Stibenz, N. Zhavoronkov, and G. Steinmeyer, Opt. Lett. **31**, 274 (2006).

[5] S. Skupin, G. Stibenz, L. Bergé, F. Lederer, T. Sokollik, M. Schnürer, N. Zhavoronkov, and G. Steinmeyer, Phys. Rev. E **74**, 056604 (2006).

[6] C. Brée, A. Demircan, and G. Steinmeyer, Laser Phys. **19**, 330 (2009).

[7] C. Brée, A. Demircan, S. Skupin, L. Bergé, and G. Steinmeyer, Opt. Express **17**, 16429 (2009).

[8] C. Brée, J. Bethge, S. Skupin, L. Bergé, A. Demircan, G. Steinmeyer, New J. Phys. **12** 093046 (2010).

[9] T. B. Benjamin and J. E. Feir, J. Fluid Mech. **27**, 417 (1967).

[10] V. I. Bespalov and V. I. Talanov, Sov. Phys. JETP **11**, 471 (1966).

[11] V. E. Zakharov, Sov. Phys. JETP **35**, 908 (1972).

[12] A. Braun, G. Korn, X. Liu, D. Du, J. Squier, and G. Mourou, Opt. Lett. **20** 73 (1995).

[13] Z. G. Ji, J. S. Liu, Z. X. Wang, J. Ju, X. M. Lu, Y. H. Jiang, Y. X. Leng, X. Y. Liang, W. Liu, S. L. Chin, R. X. Li, and Z. Z. Xu, Laser Phys. **20** 886 (2010).

[14] L. Bergé, J. J. Rasmussen, E. A. Kuznetsov, E. G. Shapiro, and S. G. Turitsyn, J. Opt. Soc. Am. B **13**, 1879 (1996).

[15] L. Bergé, K. Germaschewski, R. Grauer, and J. Juul Rasmussen, Phys. Rev. Lett. **89**, 153902 (2002).

[16] D. Faccio, M. A. Porras, A. Dubietis, F. Bragheri, A. Couairon, P. Di Trapani, Phys. Rev. Lett. **96**, 193901 (2006).

[17] A. Dalgarno and A. E. Kingston, Proc. Roy. Soc. A **259**, 424 (1960).

[18] H. J. Lehmeier, W. Leupacher, and A. Penzkofer, Opt. Commun. **56**, 67 (1985).

[19] A. M. Perelomov, V. S. Popov, M. V. Terent'ev, Sov. Phys. JETP **23**, 924 (1966).

[20] S. Skupin, U. Peschel, C. Etrich, L. Leine, F. Lederer, and D. Michaelis, Opt. Quant. Electron. **35**,573 (2003).

[21] D. Faccio, A. Averchi, A. Lotti, P. Di Trapani, A. Couairon, D. Papazoglou and S. Tzortzakis, Opt. Express **16**, 1565–1570 (2008).

[22] A. E. Dormidonov and V. P. Kandidov, Laser Phys. **19** 1993 (2009).

[23] R. Y. Chiao, E. Garmire, and C. H. Townes, Phys. Rev. Lett. **13**, 479 (1964).

[24] D. S. Steingrube, E. Schulz, T. Binhammer, T. Vockerodt, U. Morgner, and M. Kovacev, Opt. Exp. **17** 16177 (2009).

[25] T. J. Wang, J. F. Daigle, Y. Chen, C. Marceau, F. Théberge, M. Châteauneuf, J. Dubois, and S. L. Chin, Laser Phys. Lett. **7** 517 (2010).

[26] T. J. Wang, C. Marceau, S. Yuan, Y. Chen, Q. Wang, F. Théberge, M. Châteauneuf, J. Dubois, and S. L. Chin, Laser Phys. Lett., **DOI** 10.1002/lapl.201010088.